



Automation in Confocal Microscopy Detection of Cancer-Associated Fibroblast Effects on Metastasizing Prostate Cancer



Anthony Morales, Alexandria Carter, Ehsan Aalaei, Jason Deng, Dr. Michael R. King

Introduction

- Prostate cancer is the most prevalent male cancer accounting for 29% of all new cases.¹
- Localized disease maintains a 99% 5-year survival while metastatic disease survival drops to less than 30%.
- Cancer associated fibroblasts (CAFs) drive aggression through microenvironment modulation and active shielding of circulating tumor cells during metastasis.^{2,3}

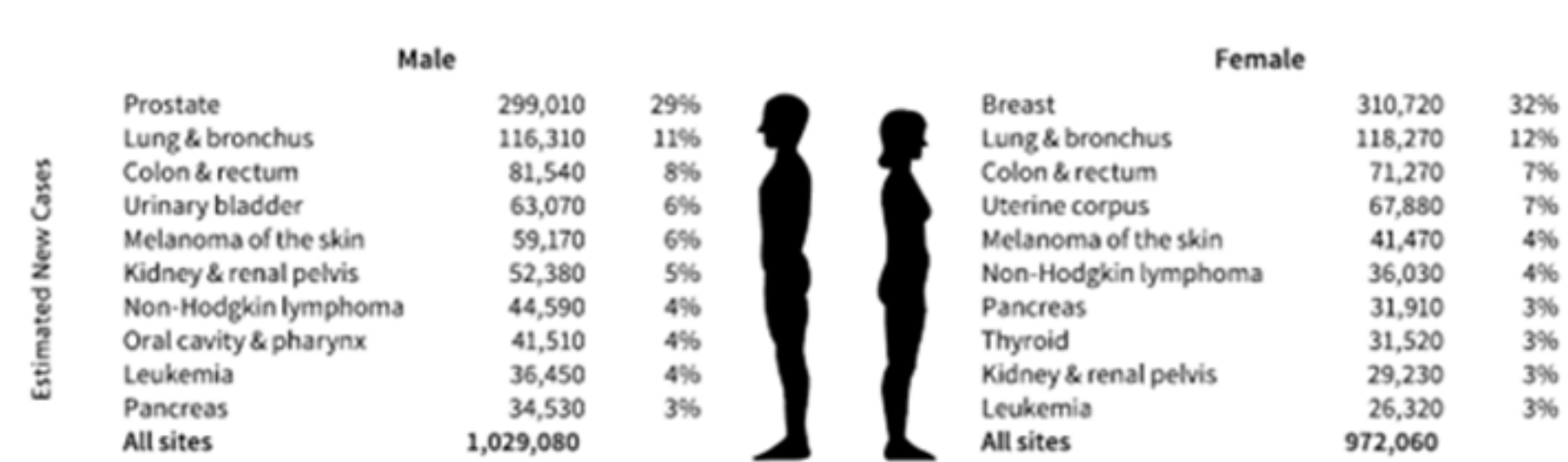


Fig. 1: ACS Cancer Estimated 2024 Incidence Statistics by Sex

Superhydrophobic Array Device

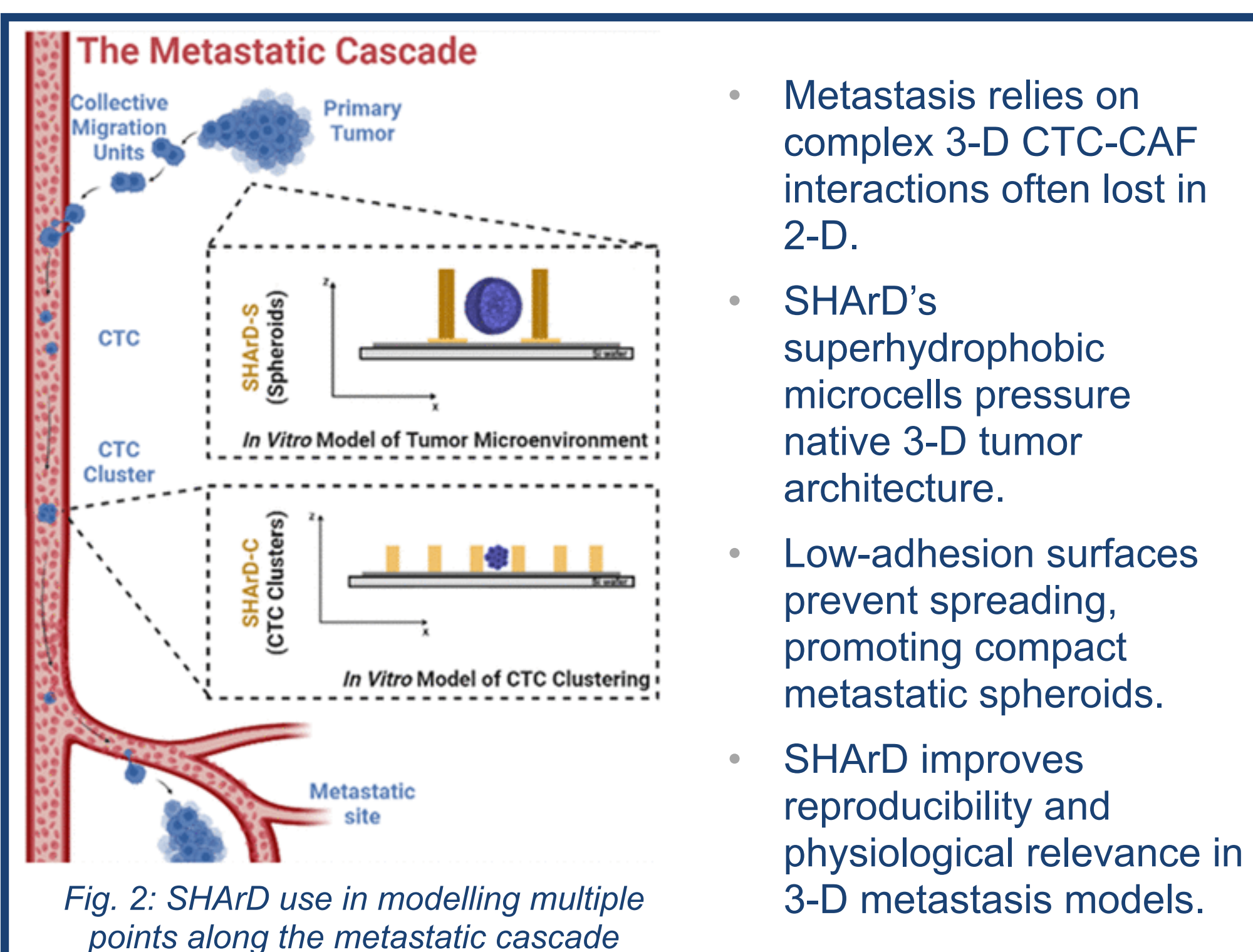


Fig. 2: SHArD use in modelling multiple points along the metastatic cascade

FABRICATION

- Deposition of a Teflon-like non-sticky polymer via plasma polymerization onto the device surface using Oxford RIE
- Build the microwell walls using thick or ultra-thick SU8 lithography to achieve 75μm or 300μm resist thickness
- Lay down a 2μm thick SU8 layer to promote adhesion of ultra-thick SU8 microwell walls or omnicoat to promote adhesion of semi-thick layer
- Anneal wafer at 500°C for 1 hour in Argon gas then grow ZnO nanorods from the nanoparticle seeds in an HMTA and Zn(NO3)2 [4]
- ZnO NP solution is sonicated with a dispersant, and spin coated onto the wafer at 1500rpm for 30 seconds

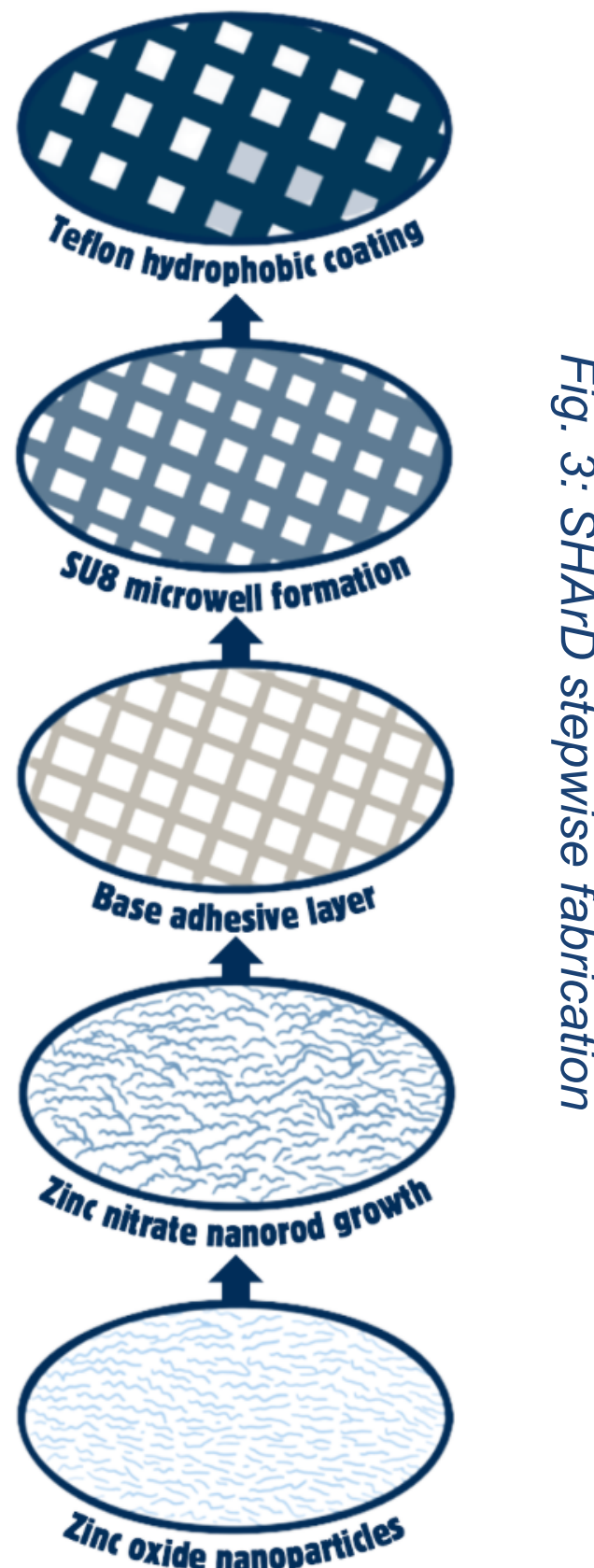
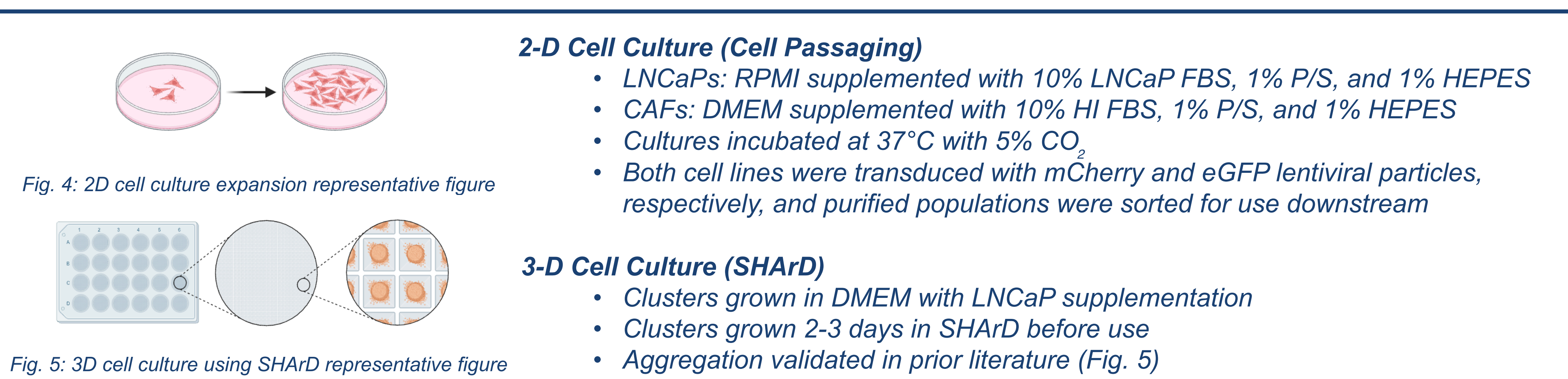


Fig. 3: SHArD stepwise fabrication

Methods



Confocal Microscopy

- CTC cluster models fixed (10% PFA), permeabilized (1% Triton), and stained
- Z-stacks captured for downstream volume and compactness analysis

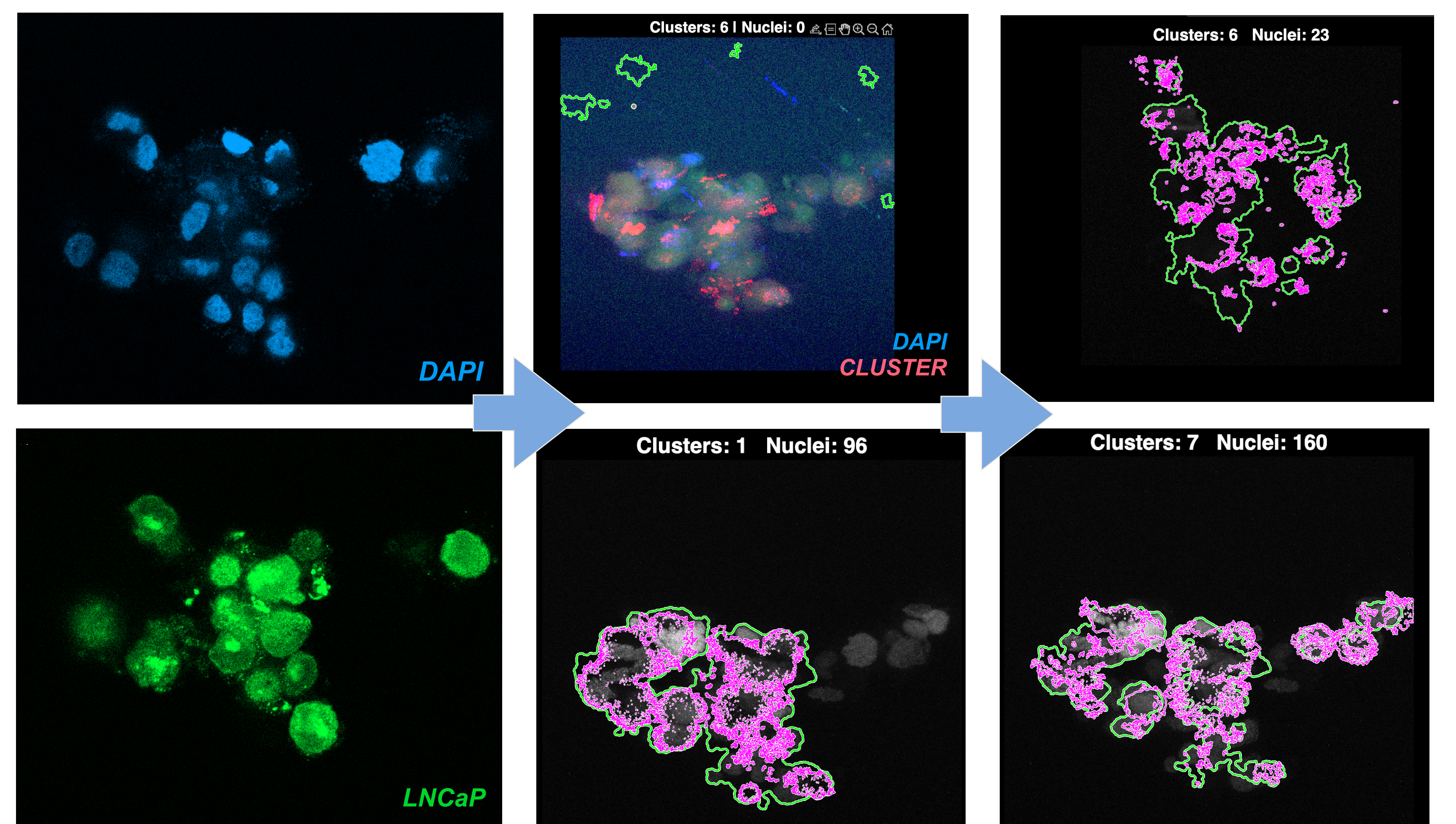
Image Analysis with FIJI

- CZI files imported and RGB channels split
- ROIs drawn to identify cluster volume and area (with edge object removal)
- Segmentation of CAF vs LNCaP pops.

Image Analysis with MATLAB

- Memory-efficient MATLAB pipeline segments 3-D nuclei and clusters
- Script outputs per-nucleus volumes and multi-channel intensity metrics

Results



- Current work with the MATLAB pipeline is designed to identify large CAF/cluster regions in 3-D stacks via CZI batch files.
- Current DAPI-based segmentation overestimates nuclei counts due to not-yet perfected filtering.
- Generated per-nucleus tables (volume, MFIs) for downstream quantitative analysis.
- MATLAB overlays provide visual QC for cluster/nuclei segmentation accuracy.

Conclusion

- Established full workflow from 3-D culture fabrication to imaging.
- Confocal imaging successfully resolved cluster organization and multi-channel spheroids.
- MATLAB pipeline produced initial 3-D nuclei and cluster quantification tables.
- Nuclei segmentation remains imperfect, as well as cluster, overcounting in dense regions.
- Pipeline already supports extraction of centroid, volume, and intensity metrics.
- Combined culture and computational workflow lays groundwork for higher throughput analysis.
- Results demonstrate feasibility of integrating engineered surfaces with computational readouts.

Future Work

- Refine DAPI thresholds, size filters, and watershed steps for accuracy.
- Improve gating to reduce false-positive nuclei in dense spheroids.
- Incorporate manual ground-truth annotations for segmentation validation.
- Benchmark MATLAB results against FIJI and CellProfiler pipelines.
- Integrate adaptive background subtraction for heterogenous z-planes.
- Automate cluster-nucleus pairing for more interpretable biological metrics.
- Expand pipeline to handle larger datasets and time-lapse imaging.
- Begin transitioning analysis pipeline for mouse-derived tumor clusters for spring project.
- Validate new 3-D culture technology clusters against mouse *in vivo* histology and morphology.
- Ultimately integrate engineered culture, mouse data, and computational analysis into a unified platform.

Acknowledgements

- Siegel RL, Miller KD, Fuchs HE, Jemal A. Cancer statistics, 2024. CA: A Cancer journal for Clinicians. 2024;74(1):7-33.
 - Nurmik M, Ullmann P, Rodriguez F, Haan S, Letellier E. In search of definitions: Cancer-associated fibroblasts and their markers. International Journal of Cancer. 2020;146(4):895-905.
 - Fukumura D, Kloepper J, Ammogzar Z, Duda DG, Jain RK. Enhancing cancer immunotherapy using antiangiogenics: opportunities and challenges. Nature Reviews Clinical Oncology. 2018;15(5):325-340.
- We acknowledge the use of the Rice Shared Equipment Authority (SEA) for access to the confocal microscopy systems used in this study. We greatly acknowledge the support of the Michael R. King Laboratory at Rice University for providing the cell lines, culture materials, licenses for FIJI and MATLAB, and access to the SHArD fabrication tools. This work would not have been possible without the contributions of these shared facilities.

Label	Centroid_x.y.z_vox_1	Centroid_x.y.z_vox_2	Centroid_x.y.z_vox_3	Voxels	ClusterID2D	MFI_Ch1	Int_Ch1	MFI_Ch2	Int_Ch2	MFI_Ch3	Int_Ch3	MFI_Ch4	Int_Ch4
1	904.722107654882	956.54731356738	7.13447598819476	80981	0	0.029485184316154	2387.73971081991	0.005898924871171	477.70104683423	0.0202036653247122	1636.11302166052	0.021884200674598	1772.54614548296
19	606.01139883375	1009.8982630273	7.40159739454094	12896	0	0.052674199620771	679.289319830947	0.00847072971876323	109.238530453171	0.086568448008433	1142.17870551675	0.080313350705989	1035.72097063492
73	975.449353574697	1120.06452521176	17.6088012388841	85238	0	0.0266198756813481	2269.02496332675	0.00778641101410309	663.698102020119	0.017489339636623	1490.79894813697	0.013701537697166	1167.85042122311
89	674.99394008421	1066.01625417681	15.0284306507334	17657	0	0.0511682544468174	903.477868767455	0.010229970493986	180.631057901231	0.0340055983578295	600.436814029549	0.0306055983578295	530.868270204195
150	768.117235547355	1128.73954489545	21.5378228782288	13008	0	0.0498669927789427	650.230802068487	0.0131204530551995	170.670853342036	0.051222794915579	666.306117250186	0.0865147137910185	1125.38339854369
193	858.396255353986	1427.26986977071	42.652106164737	290718	0	0.0508137840789948	14714.3380798772	0.0190348355366283	5533.76931753751	0.0430014745629091	12501.3026817978	0.042055006157556	1226.1472679602
210	783.39037025046	1063.63922126217	42.2750519523132	45715	0	0.0726030548345687	3319.04865176231	0.020668794057809	944.873920352738	0.0556911890085467	2545.92270552571	0.0278961512902326	1275.27255623298
264	1320.39288781996	1524.61767737502	43.6120082460058	11642	0	0.102366085345682	1191.74596559443	0.0238466808683274	277.623058696067	0.197956751779965	2304.61250422235	0.0424913540839202	494.684342449999
365	1036.99600325661	967.73408536748	42.8157797350307	40533	0	0.151200738607585	6128.61953798123	0.03288834120542	133.07500680793	0.0186310854001654	755.17378452905	0.0267400923377975	1083.85616272794

Fig 7: MATLAB output from 3-D confocal stack analysis showing per-nucleus centroid, volume, cluster assignment, and multi-channel intensity metrics extracted from CZI batch processing.